First- and second-chance proton emission in the interactions of fast neutrons with ^{92}Mo

S. M. Qaim and R. Wölfle
Institut für Chemie 1 (Nuklearchemie), Kernforschungsanlage Jülich GmbH, D-5170 Jülich, Federal Republic of Germany

Brigitte Strohmaier
Institut für Radiumforschung und Kernphysik, Universität Wien, A-1090 Vienna, Austria
(Received 23 May 1989)

Cross sections were measured radiochemically for the ^{92}Mo$(n,p)^{92}$Nb^m and ^{92}Mo$(n,n'p+pn+d)^{91}$Nb^m reactions over the neutron energy range of 9.0–10.6 MeV, and for the latter reaction also between 12.6 and 14.4 MeV. Use was made of high-resolution γ-ray and x-ray spectroscopy. Statistical-model calculations taking into account precompound effects were performed for fast neutron induced reactions on ^{92}Mo. The calculational results agree well with the experimental data on emitted proton spectra as well as on the excitation functions of various reaction channels. The second-chance proton emission is significant for incident neutron energies above 11 MeV; between 13 and 14 MeV it is comparable to the first-chance proton emission.

I. INTRODUCTION

The first-chance proton emission in fast neutron induced reactions on medium mass target nuclei has been investigated in considerable detail, both via charged particle detection (cf. Refs. 1–9) and identification of the activation product (cf. Refs. 10–13). In comparison, the second-chance proton emission processes, i.e., $(n,n'p)$, $(n,2p)$, and $(n,\alpha p)$, have received lesser attention. For excitation energies up to 20 MeV the $(n,\alpha p)$ process has not at all been observed, and the $(n,2p)$ reaction has a very low probability (cf. Ref. 14). The $(n,n'p)$ process is also expected to be rather weak since the excited levels of the (n,n') reaction product tend to deexcite via emission of a second neutron rather than a proton. Our knowledge hitherto is based on radiochemical (cf. Refs. 15–17) and charged particle detection (cf. Refs. 5–8) experiments, done mostly at 14 MeV. In target nuclei with a higher neutron separation energy than the proton separation energy ($S_n > S_p$), the second-chance proton emission competes with the second-chance neutron emission (cf. Refs. 5–8). Recently some studies were carried out on the target nuclei ^{58,60}Ni and ^{63,65}Cu at incident neutron energies of 9.4 and 11 MeV (cf. Refs. 18 and 19). For radiochemical studies at $E_n \leq 14$ MeV some of the interesting target nuclei are ^{50}Cr, ^{58}Ni, ^{92}Mo, ^{96}Ru, etc. We described earlier a study on ^{58}Ni (cf. Ref. 20). Now we choose to investigate the proton emission reactions on ^{92}Mo. Special attention was paid to the investigation of the ^{92}Mo$(n,n'p+pn+d)^{91}$Nb^m process as a function of neutron energy, with a view to determining the contribution of the second-chance proton emission.

II. EXPERIMENT

Cross sections were measured radiochemically. The pertinent techniques will be described.

A. Irradiations and neutron flux monitoring

Neutrons in the energy region ≤ 10.6 MeV were produced via the ^{2}H$(d,n)^3$He reaction using a deuterium gas target at the Jülich variable energy compact cyclotron CV28 (cf. Ref. 21). The molybdenum sample consisted of either powder filled in a polyethylene capsule (1.2 cm $\phi \times 1.3$ cm) or a stack of Mo foils (1.6 cm $\phi \times 0.8$ cm). In either case 99.9% pure material was used. Al foils of the same size as the Mo sample were attached in the front and at the back to monitor the neutron flux density. Irradiations were done in the 0° direction. The mean neutron energy for each sample was calculated using a Monte Carlo program (cf. Refs. 21 and 22). The neutron flux density effective at each sample was determined via the monitor reaction ^{27}Al$(n,\alpha)^{24}$Na (Ref. 23). In general the neutron flux density was about 4×10^7 cm^{-2} s^{-1}.

Neutrons in the energy region above 12.5 MeV were produced via the ^{3}H$(d,n)^4$He reaction using a Ti(T) solid target at the Geel CN-type Van de Graaff machine. Each sample consisted of a compact Mo disc (2 cm $\phi \times 0.5$ cm) of 99.8% purity, sandwiched between two Al monitor foils. The irradiation details are given elsewhere (cf. Ref. 13). For the present study three of those irradiated samples were treated radiochemically.

B. Radiochemical separations and source preparation

Two methods were used for the separation of niobium from irradiated molybdenum. In the first method, the molybdenum sample (3-g powder or 13-g foils) was dissolved in a mixture of concentrated H_2SO_4 and HNO_3, adding 35–80 mg Nb carrier. The solution was diluted and neutralized with NH_4OH whereby niobium was precipitated. It was washed, dissolved in a small quantity of HF, and reprecipitated with NH_4OH. The precipitate was then heated at 850 °C and weighed as Nb_2O_5. Thereafter it was transferred to an aluminum planchet, spread

over a surface of 1.8 cm ϕ, fixed with glue, and used for x-ray counting. The chemical yield was determined gravimetrically, and several months after the end of experiment, via fast neutron activation analysis using the ^{93}Nb$(n,2n)^{92}$Nb^m process. The two results agreed within 5%.

The second method of separation was used in the case of the compact molybdenum disc (15 g). The irradiated sample was placed on a very thin Nb foil (27 mg) and heated in a quartz tube in a stream of air at 1100 °C. Molybdenum was converted to MoO_3 which got sublimated. The niobium left in the tube was taken up in a mixture of dilute HF and HNO_3. Concentrated H_2SO_4 was then added to remove HF and HNO_3 and the mixture was diluted. Further treatment was then the same as described above. In this case a gravimetric determination of the chemical yield was uncertain since some radioniobium was carried over with MoO_3. The yield of niobium separation was therefore determined using ^{92}Nb^m (present in the irradiated sample) as a tracer.

C. Measurement of radioactivity

The radioactivity of the ^{92}Mo$(n,p)^{92}$Nb^m reaction product ($T_{1/2}=10.15$ d, $E_\gamma=934$ keV, $I_\gamma=99.2\%$) was determined using a 35 cm^3 Ge(Li) detector coupled to a multichannel analyzer. The count rates were corrected for self-absorption, pileup, coincidence loss, geometry, efficiency of the detector, and γ-ray abundance.

The measurement of the radioactivity of the ^{92}Mo$(n,n'p+pn+d)^{91}$Nb^m product presented some difficulty. This radioisotope decays with a half-life of 62 d via internal transition (IT) (96.6%) and electron capture (EC) (3.4%). The IT is strongly converted. A 1205 keV γ ray associated with the latter process has low and uncertain intensity ($\sim$3.4%). At $E_n \geq 12.5$ MeV the activity of ^{91}Nb^m could be measured using this γ ray (cf. Ref. 13) though with a large uncertainty. At $E_n \leq 10.6$ MeV it was mandatory to perform x-ray spectroscopy. The chemically separated thin sources were therefore counted on a Si(Li) detector. In all the niobium samples four major x rays were detected. These corresponded to the K_α and K_β x rays of niobium (16.58 and 18.62 keV) and zirconium (15.75 and 17.67 keV). The former are associated with the highly converted IT of ^{91}Nb^m to ^{91}Nb^g and the latter mainly with the EC decay of ^{92}Nb^m to ^{92}Zr. Counting was started about 20 d after the end of irradiation and the decay followed for about 200 d. The K_α x ray of zirconium decreased in intensity with a half-life of about 10.2 d and confirmed the presence of ^{92}Nb^m. The K_α x ray of niobium, however, showed two components. By subtracting the contribution of a weak uncharacterized long-lived component, the count rate of the shorter-lived activity ($T_{1/2} \approx 60$ d), attributed to ^{91}Nb^m, could be determined.

The K_α x-ray count rates of ^{92}Nb^m and ^{91}Nb^m were subjected to corrections for self-absorption, finite size of the source, efficiency of the detector, chemical yield of separation, and x-ray intensities which were 54.3$\pm$0.1 and 40.9$\pm$0.8 %, respectively (cf. Ref. 24).

The decay rates of ^{92}Nb^m determined via x-ray spectroscopy were, in general, about 15% smaller than those via γ-ray spectroscopy. This result showed that a quantitative determination of radioactivity via x-ray spectroscopy is reliable. However, due to their higher accuracy we adopted only the γ-ray spectroscopic results for calculating ^{92}Mo$(n,p)^{92}$Nb^m cross sections. In contrast, the decay rates of ^{91}Nb^m determined via x-ray spectroscopy were about 30% higher than those via γ-ray counting. Here we adopted the x-ray counting data for calculating cross sections of the ^{92}Mo$(n,n'p+pn+d)^{91}$Nb^m process, since the low and uncertain intensity of the 1205 keV γ-ray presumably involved larger errors.

D. Calculation of cross sections and errors

In studies with *dd* neutrons ($E_n \leq 10.6$ MeV) the decay rates of both ^{92}Nb^m and ^{91}Nb^m were corrected for contributions from background neutrons (gas-out–gas-in results and breakup of deuterons on D_2 gas). With *dt* neutrons ($E_n \geq 13.4$ MeV) a small correction for the formation of ^{91}Nb^m through the decay of ^{91}Mo^m [formed via the $(n,2n)$ reaction of ^{92}Mo] was necessary. From the corrected decay rates of ^{92}Nb^m and ^{91}Nb^m and the mean neutron flux densities the cross sections were calculated using the well-known activation equation.

The principal sources of error and their magnitudes in our activation cross-section measurements have been described in detail earlier (cf. Refs. 13, 21, and 22). The present studies involving x-ray spectroscopy have somewhat larger errors. Combining the individual components of error in quadrature, the total error for each cross-section value was obtained.

III. NUCLEAR MODEL CALCULATIONS

Compound nucleus model calculations were performed for particle emission from the equilibrated nuclei (width fluctuation corrected Hauser-Feshbach formula for first-chance emission, evaporation formula for higher-chance emission), and the exciton model was used to account for precompound decay. These calculations are closely related to those carried out for neutron-induced cross sections on Nb (Refs. 25–27) using the same computer code (Ref. 28). The aim of these model calculations was to describe our experimental results for the ^{92}Mo$(n,p)^{92}$Nb^m and the ^{92}Mo$(n,n'p+pn+d)^{91}$Nb^m excitation functions as well as those for other neutron induced reactions on ^{92}Mo, with a parametrization consistent with that used for a revised evaluation of Nb cross sections (Ref. 29).

In the Hauser-Feshbach calculations, discrete levels were specified according to the information from Nuclear Data Sheets (Ref. 30). We considered 16 discrete levels in ^{91}Nb (up to 2.171 MeV), 30 in ^{92}Nb (up to 1.720 MeV), 13 in ^{91}Mo (up to 2.083 MeV), and 11 in ^{92}Mo (up to 3.091 MeV). The continuum level densities were described in the frame of the back-shifted Fermi gas model. The level-density parameters were—with some modifications—those of Dilg *et al.* (Ref. 31) assuming the effective moment of inertia to be equal to the rigid body value calculated with a radius parameter of 1.25 fm. The transmission coefficients utilized in the calculations were derived from the spherical optical model, using global optical potentials for protons (Ref. 32), deuterons (Ref. 33),

and α particles (Ref. 34) and an optical potential determined originally for ^{93}Nb (Ref. 35), modified as described in Ref. 29.

For γ-ray emission, the strength functions were calculated from the Brink-Axel model for $E1$ radiation and the Weisskopf model for $M1$, $E2$, $M2$, $E3$, and $M3$ radiation. The normalization of the strength functions of all other radiation types relative to the $E1$ strength function at the neutron binding energy was guided by the ratio of local ($A \approx 90$) averages of $M1$ and $E1$ strength functions in the work by McCullagh *et al.* (Ref. 36) in the case of magnetic dipole radiation, according to Weisskopf's estimate for the higher multipole types. Finally, the strength functions of γ rays of all multipole types were normalized by the average value of the factors required for adjusting calculated neutron capture cross sections for several nuclei in the mass range $A = 88-103$ to the corresponding measured values. For ^{92}Mo, the $M1/E1$ ratio and the overall normalization factor were somewhat varied to influence the $(n,n'p)$ contribution to the proton emission spectrum at 14.8-MeV incident neutron energy, thereby achieving better agreement with the measurement of Haight *et al.* (Ref. 8). As far as the exciton model is concerned, we calculated the internal transition rates according to the formulas by Williams (Ref. 37). A value of 300 MeV^3 for the constant in the squared matrix element (Ref. 38) for internal transitions and an α-particle preformation factor of 0.14 were used. Pairing was accounted for by applying an appropriate energy shift in the particle-hole state densities (Ref. 39).

During the course of the revised neutron cross-section evaluation (Ref. 29) on ^{93}Nb, it was found necessary to consider a contribution to the neutron emission spectrum from direct inelastic scattering to levels around 2-MeV excitation energy in ^{93}Nb. This effect was accounted for by assuming an integral value of 100 mb for this direct inelastic scattering component at incident neutron energies above 8 MeV and scaling down the absorption cross section, and consequently neutron induced cross sections, by a factor

$$[\sigma_{\text{abs}}(\text{mb}) - 100]/\sigma_{\text{abs}}(\text{mb}) .$$

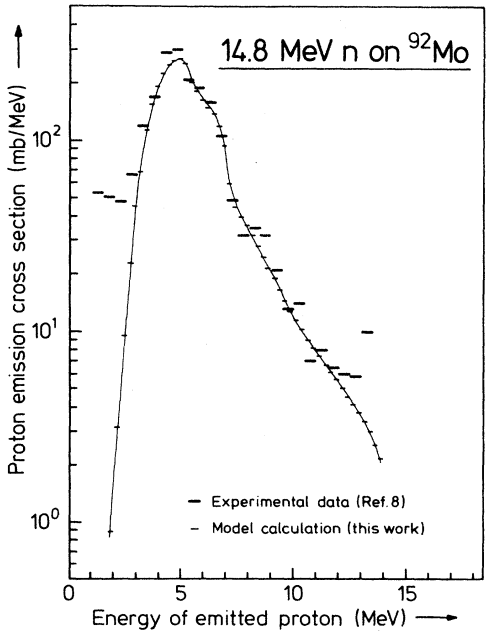

FIG. 1. Experimentally determined angle-integrated cross sections for proton emission in the interactions of 14.8-MeV neutrons on ^{92}Mo (Ref. 8), and comparison with the statistical-model calculations (this work). The curve drawn through the calculated data is an eye guide.

The same correction was applied in the present calculations on ^{92}Mo.

IV. RESULTS AND DISCUSSION

The results of measurements are presented in Table I. The total error in the ^{92}Mo$(n,p)^{92}$Nb^m reaction cross section amounts to between 8 and 10 % for $E_n \leq 10.6$ MeV, and 6.5% around 14 MeV (cf. Ref. 13). The total error in the ^{92}Mo$(n,n'p+pn+d)^{91}$Nb^m cross sections varied between 55% (near the threshold) and 11% (at 14 MeV).

As a check on the model calculations, we first discuss

TABLE I. Cross sections for the formation of ^{92}Nb^m and ^{91}Nb^m in fast neutron-induced reactions on ^{92}Mo.

Mean neutron energy effective at Mo sample[a] (MeV)	Cross section (mb) ^{92}Mo$(n,p)^{92}$Nb^m [b]	^{92}Mo$(n,n'p+pn+d)^{91}$Nb^m [c]
9.03±0.32	95±9	0.09±0.05
9.60±0.29	104±9	0.19±0.10
10.14±0.25	110±8	1.43±0.75
10.64±0.23	116±9	2.82±0.46
12.59±0.28	[d]	111±12
13.39±0.39	[d]	166±18
14.36±0.49	[d]	188±20

[a]The deviations do not give errors, they show energy spreads due to angle of emission.
[b]Results based on γ-ray spectroscopy. For details see the text.
[c]Results based on x-ray spectroscopy. For details see the text.
[d]Cross-section values reported in Ref. 13.

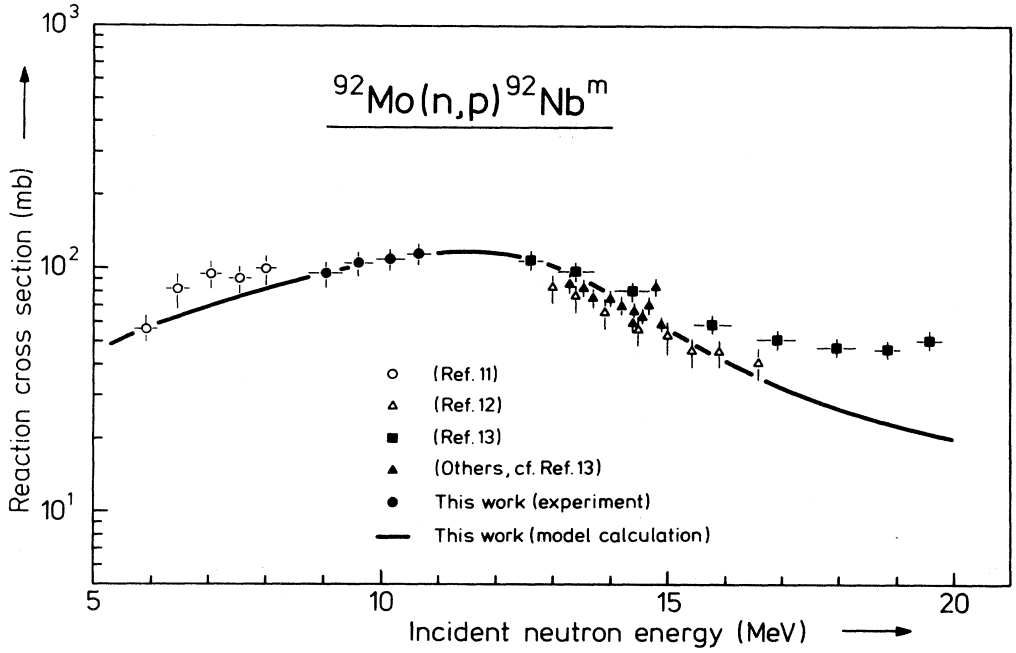

FIG. 2. Excitation function of the ^{92}Mo$(n,p)^{92}$Nb^m reaction. The curve gives the results of model calculations.

the results on the proton emission spectrum. The experimental data reported by Haight *et al.* (Ref. 8) for 14.8-MeV neutrons incident on ^{92}Mo are given in Fig. 1 together with our calculational results. Except for very high- and very low-energy protons ($E_p > 13$ MeV or $E_p = 1.0-2.0$ MeV) the agreement between experimental data and theoretical values is good. The integral over the calculated spectrum is 848 mb, in agreement with the experimental value of 967 ± 116 mb (Ref. 8). As a next step, a comparison of experimental and calculated excitation functions was undertaken. Our calculations reproduced the experimental excitation functions of ^{92}Mo$(n,2n)^{91}$Mo^{m,g} reactions given in Ref. 12 very well. Similarly the calculated excitation functions of the reactions ^{92}Mo$(n,\alpha)^{89}$Zr^{m,g} were found to be in agreement with the recent experimental data (cf. Refs. 13 and 40). The results of calculations for the ^{92}Mo$(n,p)^{92}$Nb^m reaction are shown in Fig. 2 together with the experimental data (Refs. 11–13, and this work). Some of the earlier Jülich measurements (Ref. 11) in the energy range between 8.6 and 9.6 MeV were found to be rather high and are not given in Fig. 2. It is evident that in the energy region up to 16 MeV the experimental curve is reproduced well by the calculation; beyond 16 MeV there are some deviations. This is presumably due to contributions either from direct interactions or from $(n,p2n+dn+t)$ processes on ^{94}Mo (cf. Ref. 13).

The experimental excitation function of the ^{92}Mo$(n,n'p+pn+d)^{91}$Nb^m process is shown in Fig. 3 and constitutes the first systematic study near its threshold. The model calculation gives the magnitudes of $(n,n'p)$ and (n,pn) processes, the (n,d) contribution being negligibly small over the whole energy range. The summed cross section is in excellent agreement with the experimental data at $E_n \geq 10$ MeV. At lower energies the calculated values are too low. For the product nucleus ^{91}Nb the total γ-ray strength as well as the relative strengths of $E1$ and $M1$ radiation were varied, but this did not lead to any significant improvement in the agree-

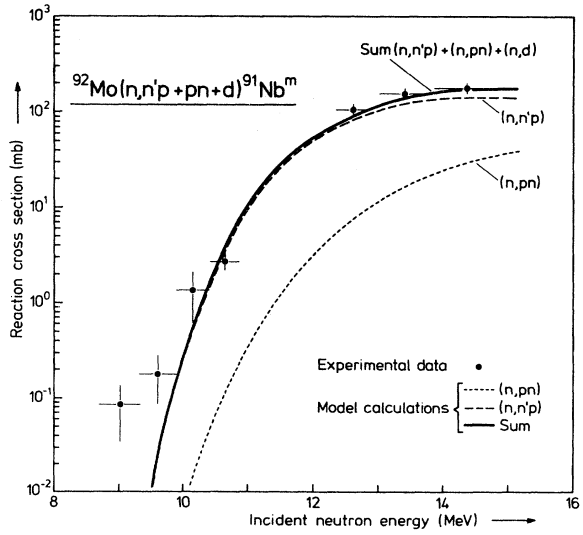

FIG. 3. Excitation function of the ^{92}Mo$(n,n'p+pn+d)^{91}$Nb^m process. The results of model calculations are given as curves: the individual $(n,n'p)$ and (n,pn) contributions are depicted as dashed curves, and the summed cross section as a solid curve. The calculated (n,d) contribution is negligible and is not shown.

ment with the measurement. No variations in the optical-model parameters were carried out apart from the modification of the neutron optical potential mentioned earlier. In fact, this modification slightly decreased the $^{91}Nb^m$ production cross section between threshold and 10 MeV and hence deteriorated the agreement between calculation and experiment, which was, however, accepted in view of the constraint on the choice of parameters consistent with those of Ref. 29. The disagreement between experiment and theory at $E_n \leq 10$ MeV may be due to the neglect of the direct interaction part in the calculation for the (n,d) reaction, which near the threshold of the $(n,n'p)$ process may be proportionally high. From charged particle emission studies (cf. Ref. 8) it is inferred that the cross section for the formation of $^{91}Nb^m$ via the (n,d) reaction on ^{92}Mo at 14.8 MeV is ~ 10 mb. The main contributing processes to the formation of $^{91}Nb^m$ are thus $(n,n'p)$ and (n,pn). The results of model calculations show that at all incident neutron energies, the $(n,n'p)$ channel is much stronger than the (n,pn) channel.

The sum of cross sections of the $^{92}Mo(n,p)^{92}Nb^m$ and $^{92}Mo(n,n'p+pn)^{91}Nb^m$ reactions obtained radiochemically in the present work amounts to about 250 mb at 14.8 MeV. This value is much smaller than the total proton emission cross section of 967 ± 116 mb reported by Haight *et al.* (Ref. 8). Presumably, in the deexcitation of $^{93}Mo^*$ greater parts of the transitions occur to $^{92}Nb^g$ and $^{91}Nb^g$ rather than to the isomeric states studied radiochemically. This is confirmed by the calculation which is reasonably compatible with both the experimental proton production and the measured production cross sections for $^{91}Nb^m$ and $^{92}Nb^m$. Unfortunately, the ground states of ^{91}Nb and ^{92}Nb are long lived (7×10^2 and 3.2×10^7 y, respectively), and no activation measurement has been reported. The results shown in Figs. 2 and 3 suggest that the second-chance proton emission is significant for incident neutron energies above 11 MeV; between 13 and 14 MeV it is comparable to the first-chance proton emission.

The Q values of the $(n,n'p)$ and $(n,2n)$ processes on ^{92}Mo are 7.6 and 12.7 MeV, respectively. Consequently, at incident neutron energies below 12.7 MeV the (n,n') reaction product can deexcite only by γ emission or second-chance proton emission. This explains the high $(n,n'p)$ cross section. Other data (cf. Refs. 12 and 13) suggest that at energies above 15 MeV the $(n,2n)$ cross section increases, resulting in the decreasing contribution of the second-chance proton emission process.

ACKNOWLEDGMENTS

We thank Professor G. Stöcklin for his active support of experimental work at Jülich and Professor H. Vonach for his interest in model calculations at Vienna. Dr. H. Liskien [Central Bureau for Nuclear Measurements (CBNM Geel)] kindly let us use the samples irradiated in Geel for chemical processing and x-ray counting. A useful discussion with Dr. W. Bambynek (CBNM Geel) on x-ray yields is gratefully acknowledged.

[1]D. L. Allan, Nucl. Phys. **24**, 274 (1961).
[2]R. N. Glover and K. H. Purser, Nucl. Phys. **24**, 431 (1961).
[3]K. R. Alvar, Nucl. Phys. **A195**, 289 (1972).
[4]J. Niidome, M. Hyakutake, N. Koori, I. Kumabe, and M. Matoba, Nucl. Phys. **A245**, 509 (1975).
[5]S. M. Grimes, R. C. Haight, and J. D. Anderson, Nucl. Sci. Eng. **62**, 187 (1977).
[6]S. M. Grimes, R. C. Haight, and J. D. Anderson, Phys. Rev. C **17**, 508 (1978).
[7]S. M. Grimes, R. C. Haight, K. R. Alvar, H. H. Barschall, and R. R. Borchers, Phys. Rev. C **19**, 2127 (1979).
[8]R. C. Haight, S. M. Grimes, R. G. Johnson, and H. H. Barschall, Phys. Rev. C **23**, 700 (1981).
[9]G. Traxler, A. Chalupka, B. Strohmaier, M. Uhl, and H. Vonach, Nucl. Sci. Eng. **90**, 174 (1985).
[10]N. I. Molla and S. M. Qaim, Nucl. Phys. **A283**, 269 (1977).
[11]M. M. Rahman and S. M. Qaim, Nucl. Phys. **A435**, 43 (1985).
[12]A. Marcinkowski, K. Stankiewicz, U. Garuska, and M. Herman, Z. Phys. A **323**, 91 (1986).
[13]H. Liskien, R. Wölfle, R. Widera, and S. M. Qaim, Appl. Radiat. Isotopes (in press).
[14]S. Lulic, P. Strohal, and I. Slaus, Nucl. Phys. **A154**, 273 (1970).
[15]W.-D. Lu and R. W. Fink, Phys. Rev. C **4**, 1173 (1971).
[16]S. M. Qaim and G. Stöcklin, Proceedings of the 8th Symposium on Fusion Technology, Noordwijkerhout, The Netherlands, 1974 (Commission of the European Communities, Luxembourg, Report EUR 5182 e, 1974, p. 939).
[17]S. M. Qaim, Nucl. Phys. **A382**, 255 (1982).
[18]S. L. Graham, M. Ahmad, S. M. Grimes, H. Satyanarayana, and S. K. Saraf, Nucl. Sci. Eng. **95**, 60 (1987).
[19]M. Ahmad, C. E. Brient, P. M. Egun, S. M. Grimes, S. Saraf, and H. Satyanarayana, Nucl. Sci. Eng. **95**, 296 (1987).
[20]S. M. Qaim and R. Wölfle, Phys. Rev. C **32**, 305 (1985).
[21]S. M. Qaim, R. Wölfle, M. M. Rahman, and H. Ollig, Nucl. Sci. Eng. **88**, 143 (1984).
[22]S. M. Qaim and R. Wölfle, Nucl. Sci. Eng. **96**, 52 (1987).
[23]S. Tagesen and H. Vonach, *Physics Data 13-3* (Fachinformationszentrum, Karlsruhe, 1981); see also H. Vonach, International Atomic Energy Agency, Technical Report Series No. 227 (IAEA, Vienna, 1983), p. 59.
[24]E. Browne and R. B. Firestone, in *Table of Radioactive Isotopes*, edited by V. S. Shirley (Wiley, London, 1986).
[25]B. Strohmaier, S. Tagesen, and H. Vonach, *Physics Data 13-2* (Fachinformationszentrum, Karlsruhe, 1980).
[26]B. Strohmaier, Ann. Nucl. Energy **9**, 397 (1982).
[27]B. Strohmaier, Proceedings of the International Atomic Energy Agency Consultants' Meeting on Nuclear Data for Structural Materials, Vienna, 1983 [IAEA Report INDC (NDS)-152/L, 1984, p. 105].
[28]M. Uhl and B. Strohmaier, Institut für Radiumforschung und Kernphysik Report IRK-76/01, 1976, and Addenda to this report (unpublished); see also B. Strohmaier and M. Uhl, Proceedings of the Winter College on Nuclear Theory for Applications, Trieste, 1978, International Atomic Energy Agency Report IAEA-SMR-43, 1980, p. 313.
[29]B. Strohmaier, Ann. Nucl. Energy (in press).
[30]*Nuclear Data Sheets* (Academic, New York, 1980), Vols. 30 and 31.
[31]W. Dilg, W. Schantl, H. Vonach, and M. Uhl, Nucl. Phys.

A217, 269 (1973).
[32]G. S. Mani, M. A. Melkanoff, and I. Iori, Commissariat à l'Energie Atomique Report CEA-2379, 1963.
[33]C. M. Perey and F. G. Perey, At. Data Nucl. Data Tables **17**, 1 (1976).
[34]J. R. Huizenga and G. Igo, Nucl. Phys. **29**, 462 (1962).
[35]J. P. Delaroche, Ch. Lagrange, and J. Salvy, Proceedings of the International Atomic Energy Agency Consultants' Meeting on the Use of Nuclear Theory in Neutron Nuclear Data Evaluation, Trieste, 1975 (IAEA Report IAEA-190, 1976, p. 251).
[36]C. M. McCullagh, M. L. Stelts, and R. E. Chrien, Phys. C **23**, 1394 (1981).
[37]F. C. Williams, Jr., Phys. Lett. **31B**, 184 (1970).
[38]C. Kalbach-Cline, Nucl. Phys. **A210**, 590 (1973).
[39]F. C. Williams, Jr., Nucl. Phys. **A166**, 231 (1971).
[40]V. McLane, C. L. Dunford, and P. F. Rose, *Neutron Cross Section Curves,* Vol. 2 of *Neutron Cross Sections* (Academic, New York, 1988).